# Electric sail trajectory correction in presence of environmental uncertainties

Andrea Caruso*, Lorenzo Niccolai, Giovanni Mengali, Alessandro A. Quarta

*Dipartimento di Ingegneria Civile e Industriale, University of Pisa, Italy*

**Abstract**

An Electric Solar Wind Sail (E-sail) is an innovative propellantless propulsion system that generates a propulsive acceleration by exchanging momentum with the solar wind charged particles. Optimal E-sail trajectories are usually investigated by assuming an average value of the solar wind characteristics, thus obtaining a deterministic reference trajectory. However, recent analyses have shown that the solar wind dynamic pressure should be modelled as a random variable and an E-sail-based spacecraft may hardly be steered toward a target celestial body in an uncertain environment with just an open-loop control law. Therefore, this paper proposes to solve such a problem with a combined control strategy that suitably adjusts the grid electric voltage in response to the measured value of the dynamic pressure, and counteracts the effects of the solar wind uncertainties by rectifying the nominal trajectory at suitably chosen points. The effectiveness of such an approach is verified by simulation using two-dimensional transfer scenarios.

*Keywords:* Electric solar wind sail, propulsive acceleration uncertainty, trajectory optimization

## Nomenclature

| | | |
|---|---|---|
| $\boldsymbol{a}$ | = | propulsive acceleration vector, $[\mathrm{mm/s^2}]$ |
| $a_c$ | = | characteristic acceleration, $[\mathrm{mm/s^2}]$ |
| $a_r$ | = | radial component of $\boldsymbol{a}$, $[\mathrm{mm/s^2}]$ |
| $a_\theta$ | = | circumferential component of $\boldsymbol{a}$, $[\mathrm{mm/s^2}]$ |
| $e$ | = | orbit eccentricity |
| $\mathcal{H}$ | = | Hamiltonian function |
| $J$ | = | performance index |
| $L$ | = | generic tether length, [km] |
| $m$ | = | spacecraft mass, [kg] |
| $N$ | = | number of tethers |
| $\hat{\boldsymbol{n}}$ | = | unit vector normal to the E-sail nominal plane |
| $O$ | = | Sun's center-of-mass |
| $p$ | = | orbit semilatus rectum, [au] |
| $p_\oplus$ | = | solar wind dynamic pressure at 1 au, [nPa] |
| $r$ | = | Sun-spacecraft distance, [au] |
| $r_\oplus$ | = | reference distance equal to 1 au |
| $\hat{\boldsymbol{r}}$ | = | radial unit vector |
| $\mathcal{T}$ | = | polar reference frame |

*Corresponding author

*Email addresses:* andrea.caruso@ing.unipi.it (Andrea Caruso), lorenzo.niccolai@ing.unipi.it (Lorenzo Niccolai), g.mengali@ing.unipi.it (Giovanni Mengali), a.quarta@ing.unipi.it (Alessandro A. Quarta)

Published in Aerospace Science and Technology, Vol. 94, November 2019, pp. 105395 (1–7). doi: https://doi.org/10.1016/j.ast.2019.105395

| | | |
|---|---|---|
| $t$ | = | time, [ days] |
| $t_{\text{end}}^{\text{d}}$ | = | final time along the deviation arc, [ days] |
| $u$ | = | radial component of velocity, [ km/s] |
| $V$ | = | grid electric voltage, [ kV] |
| $V_i$ | = | ions electric potential, [ kV] |
| $v$ | = | circumferential component of velocity, [ km/s] |
| $\alpha$ | = | pitch angle, [ deg] |
| $\alpha_\lambda$ | = | primer vector angle, [ deg] |
| $\gamma$ | = | gamma distribution |
| $\epsilon_0$ | = | vacuum permittivity, [ F/m] |
| $\theta$ | = | polar angle, [ rad] |
| $\hat{\boldsymbol{\theta}}$ | = | circumferential unit vector |
| $\boldsymbol{\lambda_v}$ | = | primer vector |
| $\{\lambda_r, \lambda_\theta, \lambda_u, \lambda_v\}$ | = | adjoint variables |
| $\mu_\odot$ | = | Sun's gravitational parameter, [ $\text{km}^3/\text{s}^2$] |
| $\sigma_\oplus$ | = | specific thrust at 1 au, [ N/m] |
| $\tau$ | = | switching parameter |
| $\omega$ | = | longitude of pericenter, [ rad] |

*Subscripts*

| | | |
|---|---|---|
| 0 | = | value at initial time |
| $f$ | = | value at final time |
| max | = | maximum allowable value |

*Superscripts*

| | | |
|---|---|---|
| $\cdot$ | = | time derivative |
| $-$ | = | nominal design value |
| $\star$ | = | optimal value |

## 1. Introduction

An Electric Solar Wind Sail (E-sail) is an innovative propellantless propulsion system that generates a propulsive thrust by exchanging momentum with the solar wind charged particles. An E-sail-based spacecraft may be used in a number of different mission scenarios, such as interplanetary transfers [1], maintenance of non-Keplerian displaced orbits, which are especially useful for continuous observation of the polar region of a planet [2], and even more exotic Solar System escape [3].

An E-sail heliocentric trajectory is often analyzed in an optimal framework, by looking for the optimal control law that minimizes the total time of flight required to reach a target celestial body [4, 5]. In a preliminary mission analysis phase, the E-sail thrust vector is usually modelled by considering the sail as an ideally flat and axially-symmetric body, and assuming average values of the solar wind characteristics. This deterministic approach enables the determination of the E-sail trajectory either by integrating the equations of motion, or by introducing some simplifying assumptions on the trajectory shape [6] or on the thrust magnitude [7]. However, the solar wind properties are subject to non-negligible variations over time [8, 9, 10, 11] and, for that reason, recent simulations suggest to describe the E-sail propulsive acceleration as a stochastic variable, rather than a deterministic one [12, 13].

A quantification of the effects of uncertainties on aircraft and spacecraft trajectory planning is a critical issue, which has been extensively investigated in the literature [14]. In a recent work by Greco et al. [15], an extension of a direct multiple-shooting method has been introduced to deal with optimal control problems in the presence of uncertainties. Ross et al. [16] defined a Lebesgue-Stieltjes optimal control problem to compute an open-loop control law able to steer a spacecraft toward a target state in uncertain environments. Sun et al. [17] proposed a combination of differential algebra and Gaussian mixture model method for uncertainty propagation, which was shown to be able to capture possible non-Gaussianity in uncertainty propagation through non-linear dynamics.

In the specific context of E-sail-based trajectories, Niccolai et al. [12] proposed to account for the solar wind fluctuations by modelling the dynamic pressure as a random variable with a gamma probability density function (PDF). They also showed, using a simple test case with a Sun-facing sail, that the uncertainty in the spacecraft state is non-negligible even after one half revolution around the Sun only. This means that the spacecraft cannot be steered toward a target state in an uncertain environment, by means of an open-loop control law. The proposed solution for that problem was the introduction of a control law aimed at adjusting the E-sail grid voltage in response to the dynamic pressure fluctuations (measured by a sensor onboard the spacecraft), in such a way as to maintain the E-sail propulsive characteristics equal to a given design value. However, due to the constraint on the maximum allowable value of the grid electric voltage, the spacecraft may not be able to follow the nominal optimal reference trajectory.

This paper proposes a possible solution for such a problem. In essence, the idea is to update the control law that steers the spacecraft toward the target orbit as soon as the spacecraft departs from the nominal reference trajectory. The new rectified trajectory is calculated by solving an optimal problem with an indirect approach.

The paper is organized as follows. The next section introduces the mathematical model used to compute the E-sail trajectory. Section 3 describes the indirect method that generates the initial nominal reference trajectory. Then, a sort of rectification method is introduced, which is finally applied in Section 4 to two-dimensional cases involving Earth-Mars and Earth-Apophis transfers.

## 2. Problem description

Consider an E-sail-based spacecraft that initially covers a heliocentric elliptic orbit of semilatus rectum $p_0$ and eccentricity $e_0$. The mission aim is to transfer the spacecraft to a coplanar, target orbit of semilatus rectum $p_f$, eccentricity $e_f$ and longitude of pericenter $\omega_f \in [0, 2\pi)$ rad, the latter being the angle between the Sun-pericenter line of the two orbits measured counterclockwise from the apse line of the initial orbit; see Fig. 1.

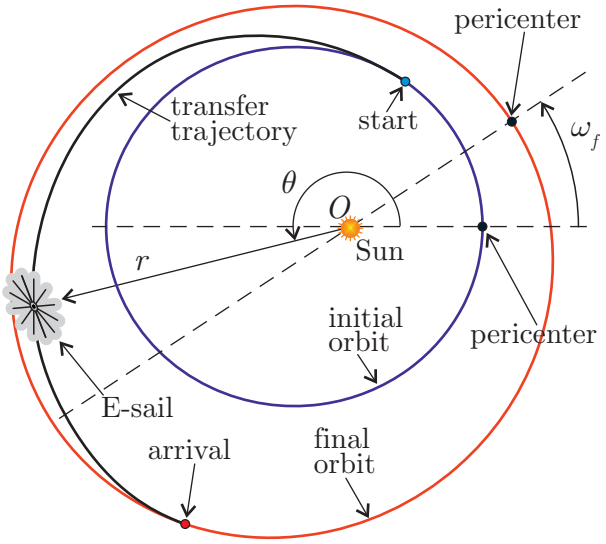


Figure 1: Reference frame and geometry of the problem.

The heliocentric motion of the spacecraft is conveniently described by introducing a polar reference frame $\mathcal{T}(O; r, \theta)$, in which $O$ is the Sun's center-of-mass, $r$ is the Sun-spacecraft distance, and $\theta$ is the polar angle measured counterclockwise from the Sun-pericenter direction of the initial orbit; see also Fig. 1. The

spacecraft equations of motion in $\mathcal{T}$ are

$$\dot{r} = u \tag{1}$$

$$\dot{\theta} = \frac{v}{r} \tag{2}$$

$$\dot{u} = -\frac{\mu_\odot}{r^2} + \frac{v^2}{r} + a_r \tag{3}$$

$$\dot{v} = -\frac{u\,v}{r} + a_\theta \tag{4}$$

where the dot symbol denotes a derivative taken with respect to time, $u$ and $v$ are the radial and circumferential components of the spacecraft velocity, $\mu_\odot$ is the Sun's gravitational parameter, while $a_r$ and $a_\theta$ are the components of the E-sail propulsive acceleration along the radial (with unit vector $\hat{\boldsymbol{r}}$) and circumferential (with unit vector $\hat{\boldsymbol{\theta}}$) directions, respectively.

Using the recent model proposed by Huo et al. [18], the propulsive acceleration vector $\boldsymbol{a}$ for a flat and axially-symmetric E-sail can be written as

$$\boldsymbol{a} = \tau \frac{a_c\, r_\oplus}{2\, r}\, \left[\hat{\boldsymbol{r}} + (\hat{\boldsymbol{r}} \cdot \hat{\boldsymbol{n}})\, \hat{\boldsymbol{n}}\right] \tag{5}$$

where $\tau \in \{0, 1\}$ is a dimensionless variable that models the possibility of switching the electron gun either on ($\tau = 1$) or off ($\tau = 0$), and $\hat{\boldsymbol{n}}$ is the unit vector normal to the E-sail nominal plane in the direction opposite to the Sun. In Eq. (5), $a_c$ is the characteristic acceleration, defined as the maximum propulsive acceleration magnitude provided by the E-sail at a reference distance $r_\oplus = 1\,\text{au}$ from the Sun. According to Ref. [18], the characteristic acceleration can be written as a function of the E-sail design parameters as

$$a_c = \frac{NL\sigma_\oplus}{m} \tag{6}$$

where $N$ is the number of tethers, $L$ is the generic tether length, $m$ is the total spacecraft mass, and $\sigma_\oplus$ is the thrust per unit of tether length generated by the E-sail. Bearing in mind the analysis of Toivanen and Janhunen [19, 20], if $r \simeq r_\oplus$ the specific thrust $\sigma_\oplus$ can be written in a compact form as

$$\sigma_\oplus = 0.18\ \max(0, V - V_i)\, \sqrt{\epsilon_0\, p_\oplus} \tag{7}$$

where $\epsilon_0$ is the vacuum permittivity, $p_\oplus$ is the dynamic pressure of the solar wind measured at a solar distance of $r = r_\oplus$, $V$ is the E-sail grid voltage, and $V_i$ is the electric potential of the ions which is about $1\,\text{kV}$. Taking into account that $V$ is usually on the order of some tens of kV, Eq. (7) simplifies to

$$\sigma_\oplus = 0.18\, V\, \sqrt{\epsilon_0\, p_\oplus} \tag{8}$$

Accordingly, from Eqs. (5)-(6) and (8), the components of the propulsive acceleration $\boldsymbol{a}$ along the radial (i.e. $a_r$) and circumferential (i.e. $a_\theta$) directions are

$$a_r \triangleq \boldsymbol{a} \cdot \hat{\boldsymbol{r}} = \tau\, \frac{0.18\, N\, L\, V}{2\, m}\, \sqrt{\epsilon_0\, p_\oplus}\, \left(\frac{r_\oplus}{r}\right)\, \left(1 + \cos^2\alpha\right) \tag{9}$$

$$a_\theta \triangleq \boldsymbol{a} \cdot \hat{\boldsymbol{\theta}} = \tau\, \frac{0.18\, N\, L\, V}{2\, m}\, \sqrt{\epsilon_0\, p_\oplus}\, \left(\frac{r_\oplus}{r}\right)\, \cos\alpha\, \sin\alpha \tag{10}$$

where $\alpha \in [-90,\, 90]\,\text{deg}$ is the sail pitch angle, defined as the angle between the direction of $\hat{\boldsymbol{r}}$ and the direction of $\hat{\boldsymbol{n}}$; see Fig. 2.

In a preliminary mission analysis phase, the E-sail heliocentric transfer trajectory is typically calculated by assuming an average value of the solar wind characteristics. In particular, the value of $p_\oplus$ is taken as constant and equal to its mean value, $\bar{p}_\oplus = 2\,\text{nPa}$. In that case, when the control law $\{\tau, \alpha\}$ is known, the spacecraft trajectory may be obtained through a numerical integration of the equations of motion (1)-(4),

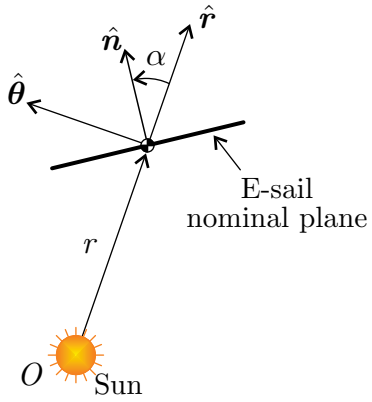


Figure 2: Sail pitch angle $\alpha$.

starting from the initial conditions associated to the parking orbit, that is

$$r(t_0) = \frac{p_0}{1 + e_0 \cos\theta_0} \tag{11}$$

$$u(t_0) = \sqrt{\frac{\mu_\odot}{p_0}}\, e_0 \, \sin\theta_0 \tag{12}$$

$$v(t_0) = \sqrt{\frac{\mu_\odot}{p_0}}\, (1 + e_0 \cos\theta_0) \tag{13}$$

where $t_0 \triangleq 0$ is the initial time, and $\theta_0 \in [0,\, 2\pi)\,\mathrm{rad}$ is the polar angle at departure, which coincides with the spacecraft true anomaly along the initial orbit.

A more reliable analysis, however, requires the effects of the solar wind uncertainties on the spacecraft trajectory to be taken into account. Because in this work two-dimensional transfers are assumed, the possible variations of $p_\oplus$ with the latitude are not considered [11]. Nevertheless, the solar wind properties are subject to non negligible variations over time [8]. For example, Fig. 3 shows the hourly fluctuations of the solar wind dynamic pressure at a Sun-spacecraft distance of 1 au, within a time span from January 1996 to September 2013. These data suggest the E-sail propulsive acceleration to be handled as a stochastic variable rather than a deterministic one. This is indeed the approach pursued by Niccolai et al. [12], who suggested to model the dynamic pressure as a random variable with a gamma distribution, in the form

$$\gamma(p_\oplus) = \frac{p_\oplus^{A-1}}{B^A\,\Gamma(A)}\, \exp\left(-p_\oplus/B\right) \tag{14}$$

with parameters $A = 1.6437$ and $B = 1.2168$. The probability density function of $p_\oplus$ is shown in Fig. 4.

The following section proposes a possible procedure to investigate optimal (minimum-time) E-sail transfer trajectories, which takes into account the uncertainties on the solar dynamic pressure.

## 3. Trajectory optimization

The heliocentric transfer problem of an E-sail-based spacecraft is usually studied within an optimal framework, by looking for the optimal control law $\tau = \tau^\star(t)$ and $\alpha = \alpha^\star(t)$ that minimizes the flight time $t_f$. As long as $p_\oplus$ is taken constant and equal to its mean value $\bar{p}_\oplus = 2\,\mathrm{nPa}$, the spacecraft characteristic acceleration has a constant value given by [12]

$$\bar{a}_c = \frac{0.18\, N\, L\, \bar{V}}{m} \sqrt{\epsilon_0\, \bar{p}_\oplus} \tag{15}$$

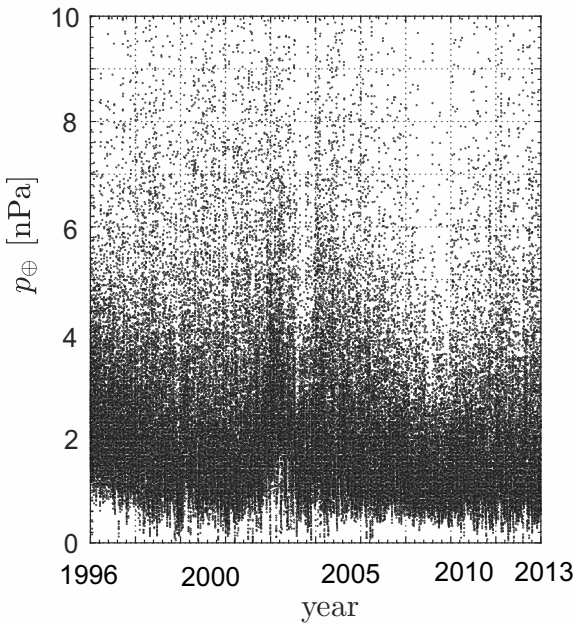


Figure 3: Hourly variation of $p_\oplus$ from January 1996 to September 2013. Data from NASA and figure adapted from Ref. [12].

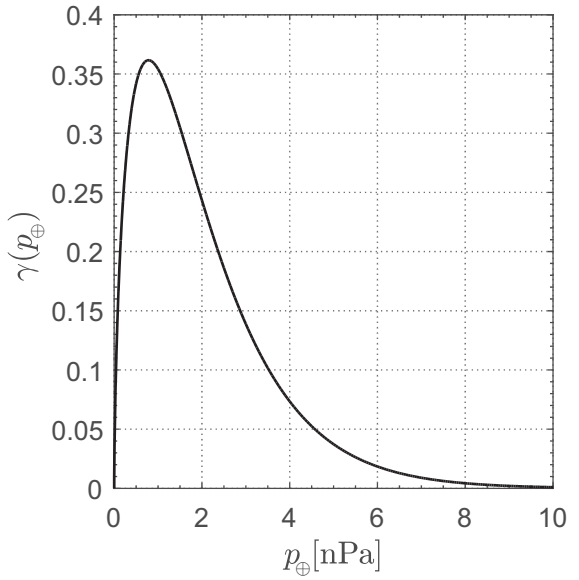


Figure 4: Probability density function of $p_\oplus$. Figure adapted from Ref. [12].

where $\bar{V}$ is the nominal design value of the grid electric voltage. The resulting optimization problem is therefore deterministic, and amounts to maximizing the performance index

$$J \triangleq -t_f \tag{16}$$

subject to the equations of motion (1)-(4), to the boundary constraints at the initial time, given by Eqs. (11)-(13), and at the final time $t_f$, that is

$$r(t_f) = \frac{p_f}{1 + e_f \cos(\theta_f - \omega_f)} \tag{17}$$

$$u(t_f) = \sqrt{\frac{\mu_\odot}{p_f}}\, e_f \sin(\theta_f - \omega_f) \tag{18}$$

$$v(t_f) = \sqrt{\frac{\mu_\odot}{p_f}}\, (1 + e_f\, \cos(\theta_f - \omega_f)) \tag{19}$$

where $\theta_f$ is the polar angle at $t_f$. Note that both the values of $\theta_0$ and $\theta_f$ are left unconstrained.

This problem may be solved with an indirect method [21]. To that end, introduce the adjoint variables $\lambda_r$, $\lambda_\theta$, $\lambda_u$ and $\lambda_v$ associated to the state variables $r$, $\theta$, $u$ and $v$, respectively. The corresponding Hamiltonian function is

$$\mathcal{H} = \lambda_r u + \lambda_\theta \frac{v}{r} + \lambda_u \left( -\frac{\mu_\odot}{r^2} + \frac{v^2}{r} + a_r \right) + \lambda_v \left( -\frac{u\, v}{r} + a_\theta \right) \tag{20}$$

Using the Euler-Lagrange equations [21], the derivatives of the adjoint variables are

$$\dot{\lambda}_r = -\frac{\partial \mathcal{H}}{\partial r} = \lambda_\theta \frac{v}{r^2} + \lambda_u \left( \frac{v^2}{r^2} - \frac{2\mu_\odot}{r^3} + \frac{a_r}{r} \right) + \lambda_v \left( -\frac{uv}{r^2} + \frac{a_\theta}{r} \right) \tag{21}$$

$$\dot{\lambda}_\theta = -\frac{\partial \mathcal{H}}{\partial \theta} = 0 \tag{22}$$

$$\dot{\lambda}_u = -\frac{\partial \mathcal{H}}{\partial u} = -\lambda_r + \lambda_v \frac{v}{r} \tag{23}$$

$$\dot{\lambda}_v = -\frac{\partial \mathcal{H}}{\partial v} = -\frac{\lambda_\theta}{r} - 2\,\lambda_u \frac{v}{r} + \lambda_v \frac{u}{r} \tag{24}$$

where $a_r$ and $a_\theta$ are given by Eqs. (9)-(10), with $p_\oplus = \bar{p}_\oplus$ and $V = \bar{V}$. Note that, from Eq. (22), the adjoint variable $\lambda_\theta$ is a constant of motion.

According to Ref. [18], the optimal control law that maximizes the Hamiltonian function at each time instant is

$$\tau^\star = \frac{1 + \text{sign}(1 + 3\cos\alpha_\lambda)}{2} \tag{25}$$

$$\alpha^\star = \frac{\alpha_\lambda}{2} \tag{26}$$

where $\text{sign}(\cdot)$ is the signum function, whereas $\alpha_\lambda \in [-180,\, 180]\,\text{deg}$ is the angle between the radial unit vector $\hat{\boldsymbol{r}}$ and $\boldsymbol{\lambda} \triangleq [\lambda_u,\, \lambda_v]^{\mathrm{T}}$, the latter being the Lawden's primer vector [22].

The minimum time trajectory is the solution of a two-point boundary value problem (TPBVP), constituted by the equations of motion (1)-(4), the Euler-Lagrange equations (21)-(24), with initial boundary conditions (11)-(13), final boundary conditions (17)-(19), and transversality conditions [21]

$$\lambda_\theta(t_0) = -\lambda_r(t_0) \frac{p_0 e_0 \sin\theta_0}{(1 + e_0 \cos\theta_0)^2} - \lambda_u(t_0) \sqrt{\frac{\mu_\odot}{p_0}} e_0 \cos\theta_0 + \lambda_v(t_0) \sqrt{\frac{\mu_\odot}{p_0}} e_0 \sin\theta_0 \tag{27}$$

$$\lambda_\theta(t_f) = -\lambda_r(t_f) \frac{p_f e_f \sin(\theta_f - \omega_f)}{(1 + e_f \cos(\theta_f - \omega_f))^2} - \lambda_u(t_f) \sqrt{\frac{\mu_\odot}{p_f}} e_f \cos(\theta_f - \omega_f) + \lambda_v(t_f) \sqrt{\frac{\mu_\odot}{p_f}} e_f \sin(\theta_f - \omega_f) \tag{28}$$

$$\mathcal{H}(t_f) = 1 \tag{29}$$

The solution to such a TPBVP coincides with the reference trajectory that would be tracked by the spacecraft in the nominal case, when $p_\oplus = \bar{p}_\oplus$. However, the uncertainties on the actual value of the solar wind dynamic pressure prevent the spacecraft to reach the target state. This problem may be solved with the aid of a control law that suitably adjusts the tether voltage, as is now shown.

*3.1. Reference trajectory rectification*

Niccolai et al. [12] suggested a possible control strategy to track the nominal trajectory in the presence of dynamic pressure fluctuations. Under the assumption that the spacecraft is able to measure the local value of the solar wind dynamic pressure $p(t)$, the grid electric voltage $V$ is adjusted [12] in such a way that the spacecraft characteristic acceleration meets its nominal value $\bar{a}_c$ given by Eq. (15). The required value of the grid voltage is therefore

$$V_{\rm req} = \frac{m\bar{a}_c}{0.18\, N\, L\, \sqrt{\epsilon_0\, p_\oplus(t)}} \tag{30}$$

with $p_\oplus(t) = p(t)\,(r/r_\oplus)^2$. Because the grid voltage $V(t)$ cannot exceed a maximum value $V_{\rm max}$, the control law is defined as

$$V(t) = \begin{cases} V_{\rm req}(t) & \text{if} \quad V_{\rm req}(t) < V_{\rm max} \\ V_{\rm max} & \text{if} \quad V_{\rm req}(t) \geq V_{\rm max} \end{cases} \tag{31}$$

Note that the control variables $\tau$ and $\alpha$ are exactly the same as those in the nominal case (that is, obtained by solving the previous TPBVP). Also note that, as long as $\tau = 0$, the spacecraft trajectory presents a Keplerian arc. In that case, there is no need to use the control law (31) because, as the E-sail thrust is off, the spacecraft covers the reference trajectory for any value of $p_\oplus$.

The whole reference trajectory (calculated with $p_\oplus = \bar{p}_\oplus$) is first partitioned into a certain number of arcs. Within each arc, the value of the solar wind dynamic pressure is maintained constant and equal to that randomly generated with a gamma distribution (14), while the grid voltage is varied in accordance with Eqs. (30)-(31). As long as $V_{\rm req} < V_{\rm max}$, the spacecraft characteristic acceleration along the arc is equal to its nominal value $\bar{a}_c$, and the spacecraft is able to track the nominal optimal trajectory. However, when the dynamic pressure becomes very small, the grid voltage $V_{\rm req}$ needs to much increase its value to generate a sufficient thrust, with a possible saturation problem. In that case, according to Eq. (31), the grid voltage is set equal to $V_{\rm max}$, but, since the E-sail characteristic acceleration is less than its nominal value (that is, $a_c < \bar{a}_c$), the spacecraft cannot track its reference trajectory. At the end of such an arc (referred to as deviation arc), the state vector is therefore different from its nominal value; see Fig. 5.

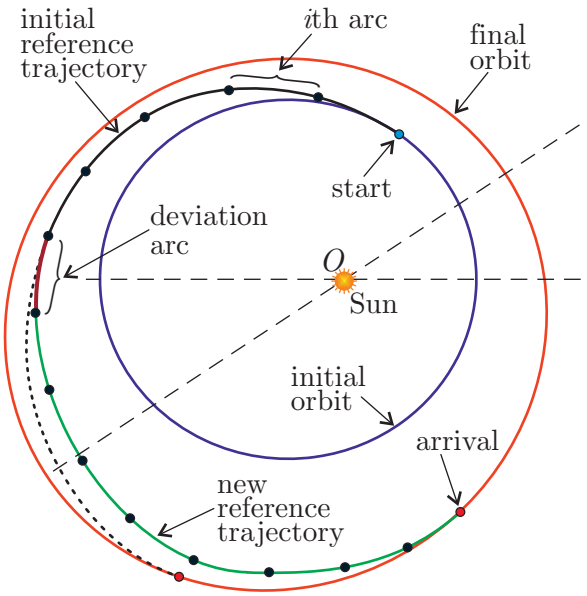


Figure 5: Deviation arc and generation of the new reference trajectory.

This problem may be circumvented by a rectification of the reference trajectory. This amounts to generating a new optimal trajectory (starting from the spacecraft state at the end of a deviation arc), which

steers the spacecraft toward the final orbit, as is shown in Fig. 5, assuming again a constant value of $p_\oplus = \bar{p}_\oplus$. Accordingly, a new optimal control problem arises, in which the performance index to maximize is

$$J_{\text{corr}} = -\left(t_f - t^{\text{d}}_{\text{end}}\right) \tag{32}$$

where $t^{\text{d}}_{\text{end}}$ is the initial time along the new reference trajectory, which coincides with the time at the end of the deviation arc. In this case, the spacecraft initial conditions are

$$r\left(t^{\text{d}}_{\text{end}}\right) = r^{\text{d}}_{\text{end}}, \quad \theta\left(t^{\text{d}}_{\text{end}}\right) = \theta^{\text{d}}_{\text{end}}, \quad u\left(t^{\text{d}}_{\text{end}}\right) = u^{\text{d}}_{\text{end}}, \quad v\left(t^{\text{d}}_{\text{end}}\right) = v^{\text{d}}_{\text{end}} \tag{33}$$

where $\{r^{\text{d}}_{\text{end}}, \theta^{\text{d}}_{\text{end}}, u^{\text{d}}_{\text{end}}, v^{\text{d}}_{\text{end}}\}$ are the state variables of the spacecraft at the end of the deviation arc. The final boundary conditions are the same as those expressed by Eqs. (17)-(19), where $\theta_f$ is again left unconstrained. In other terms, the spacecraft is subject to the dynamical equations (1)-(4), and to the Euler-Lagrange equations (21)-(24), while the resulting TPBVP is completed by the transversality conditions (28)-(29).

The solution to such a TPBVP gives a new reference trajectory (and a new optimal control law $\{\tau^\star, \alpha^\star\}$), which is tracked by the spacecraft from $t = t^{\text{d}}_{\text{end}}$ until a new deviation arc arises, when $a_c < \bar{a}_c$. The previous procedure is repeated until the spacecraft reaches the target orbit.

### *3.2. Comments*

The strategy discussed so far to perform a time-optimal transfer with an E-sail assumes that the nominal grid voltage $\bar{V}$ is a fixed parameter, which is maintained constant throughout the orbital transfer. However, some additional considerations are useful on this point. In general, the closer the nominal voltage $\bar{V}$ to the saturation voltage $V_{\max}$, the smaller the thrust modulation capability of the E-sail. Indeed, a higher reserve thrust (which corresponds to the thrust that could be obtained by increasing the voltage from the nominal to the maximum value) assures a lower risk of missing the target orbit due to solar wind fluctuations, but this comes at the cost of increasing the mission times.

An alternative strategy may be conceived by observing that the environmental uncertainty effects are more difficult to counteract in the final phase of the orbital transfer, when an accurate thrust modulation is required to reach the target orbit. Therefore, a high thrust could be generated in the early phase of the transfer by using a large nominal voltage, and then decreased in the last transfer phase to guarantee a higher reserve thrust, in order to reach the target object with an elevated confidence level. In that way, it could be possible to effectively counteract the environmental uncertainties when they are more dangerous (i.e., in the terminal transfer phase), without significantly sacrificing the E-sail performance. Such a strategy may be investigated as a possible extension of this work, and is therefore left to future research.

## 4. Numerical simulations

In this section some numerical examples are given, where the optimal transfer trajectory is obtained taking into account the presence of uncertainties in the solar wind dynamic pressure. A simplified Earth-Mars and an Earth-Apophis transfer are investigated using the method described in the previous section. In particular, the equations of motion (1)-(4) and the Euler-Lagrange equations (21)-(24) are integrated by means of a variable-step Adams-Bashforth-Moulton solver scheme [23, 24] with absolute and relative errors of $10^{-12}$.

In the following discussion, the spacecraft is propelled by an E-sail with a total number of tethers $N = 62$, each one of length $L = 19.4\,\text{km}$. The nominal grid voltage is $25\,\text{kV}$, and the total spacecraft mass is about $m = 700\,\text{kg}$ [25]. Note that, in the ideal case of $p_\oplus = \bar{p}_\oplus$, such a configuration has a nominal characteristic acceleration $\bar{a}_c = 1\,\text{mm/s}^2$.

### *4.1. Earth-Mars transfer*

An Earth-Mars transfer is first analyzed, assuming the orbit of both Earth and Mars to be coplanar. The spacecraft initially covers an orbit coincident with that of the Earth (with $p_0 = 1\,\text{au}$ and $e_0 = 0.0167$), and must be transferred to a (coplanar) final orbit coinciding with that of Mars ($p_f = 1.524$, $e_f = 0.0934$, and $\omega_f = 233.1\,\text{deg}$).

The nominal optimal trajectory (in the case of $p_\oplus = \bar{p}_\oplus$) is first computed, and the total transfer time is found to be $465.37\,\text{days}$. The whole trajectory is then partitioned into 1800 arcs, each one with a length

of about 6.2 hours, and assuming a maximum grid voltage $V_{\max} = 80\,\text{kV}$. Along each arc, a value of $p_\oplus$ is generated with the gamma PDF of Eq. (14), and each time the required grid voltage $V_{\text{req}}$ exceeds $V_{\max}$, the spacecraft trajectory deviates from the nominal optimal one. In that case, a reference trajectory rectification is obtained by computing a new reference path and the corresponding control law that steers the spacecraft toward the final orbit, as previously described.

At each run, a different control law is calculated, since the latter depends on the random values of $p_\oplus$ generated according to its PDF. However, the numerical simulations show no significant differences between the nominal optimal trajectory (obtained without dynamic pressure fluctuations) and the trajectory generated by the rectification approach (which, instead, accounts for uncertainties). The latter requires a small increase of the total flight time, on the order of a few tens of hours only. An example is shown in Fig. 6, where the flight time increase is about $\Delta t_{\text{inc}} = 25.32\,\text{hours}$.

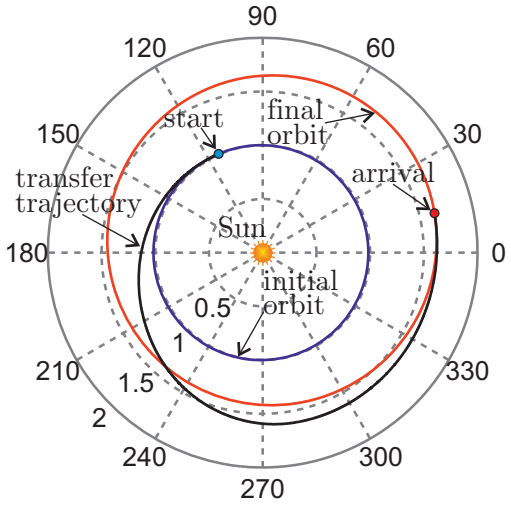


Figure 6: Optimal Earth-Mars trajectory.

Figures 7-8 also show the optimal control law $\{\tau^\star, \alpha^\star\}$ in both cases with (solid line) or without (dashed line) uncertainties in the value of $p_\oplus$. Note that, even though a small deviation of the optimal value of $\alpha^\star$ arises, the optimal control $\tau^\star$ in both cases is the same. Figure 8 also shows that, in the initial phase of the transfer, the deviation in the pitch angle $\alpha^\star$ is very small, while it tends to increase when the spacecraft approaches the target orbit.

### *4.2. Transfer toward asteroid 99942 Apophis*

Consider now a simplified transfer toward the asteroid 99942 Apophis. Again, the spacecraft initial orbital parameters are $p_0 = 1\,\text{au}$ and $e_0 = 0.0167$. The orbital inclination of Apophis with respect to the ecliptic plane (about 3.3 deg) is neglected, while the other orbital parameters are $p_f = 0.8891\,\text{au}$, $e_f = 0.1912$ and $\omega_f = 227.9\,\text{deg}$.

The transfer time along the optimal nominal trajectory is about 83.1 days. The trajectory is then partitioned into 300 arcs of about 6.6 hours each. The optimal trajectory is shown in Fig. 9, while Figs. 10-11 show the effect of the uncertainties on the optimal control law. In this example, the time increment is $\Delta t_{\text{inc}} = 11.39\,\text{hours}$.

Again, no substantial differences can be observed in both the trajectories and the control laws involving $\tau^\star$, whereas the value of $\alpha^\star$ deviates from the nominal one to steer the spacecraft towards the target orbit.

## 5. Conclusions

This work has proposed a possible strategy to generate an optimal trajectory to transfer an E-sail-based spacecraft from a parking orbit toward an elliptic orbit, while taking into account the uncertainties in the solar wind dynamic pressure. Assuming the spacecraft to be able to measure the instantaneous value of

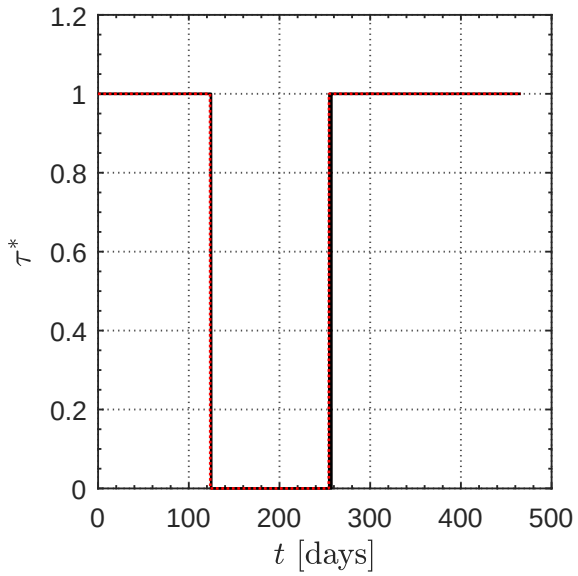


Figure 7: Earth-Mars transfer: optimal control law $\tau^\star$ in the case with uncertainties in the value of $p_\oplus$ (solid line), and in the nominal case of constant $p_\oplus = \bar{p}_\oplus$ (dashed red line).

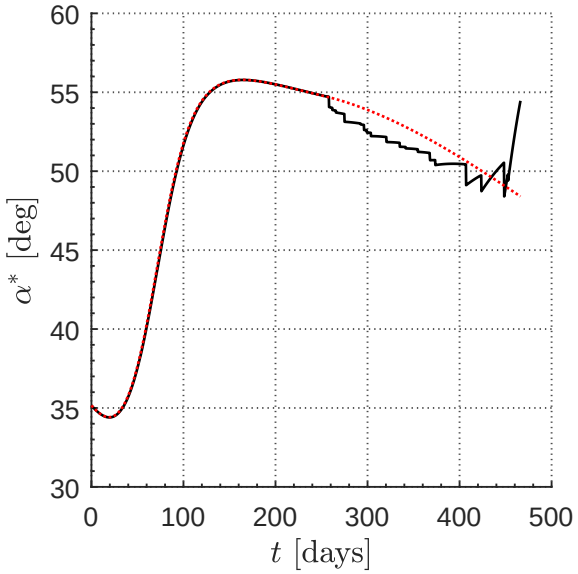


Figure 8: Earth-Mars transfer: optimal control law $\alpha^\star$ in the case of uncertainties in the value of $p_\oplus$ (solid line), and in the nominal case of constant $p_\oplus = \bar{p}_\oplus$ (dashed red line).

the local solar wind dynamic pressure, the grid voltage is varied such that the characteristic acceleration equals its nominal design value. Since the grid electric voltage cannot exceed a maximum allowable value, as soon as a saturation occurs, the spacecraft departs from its nominal trajectory, and a course correction is necessary for the spacecraft to reach the target orbit. Every time such a deviation from the reference trajectory takes place, the control law that steers the spacecraft toward the final orbit is updated, and a new reference trajectory is generated. From the numerical simulations, a minor increase in the time of flight is observed when compared to the nominal optimal trajectory, while a small pitch angle correction is sufficient

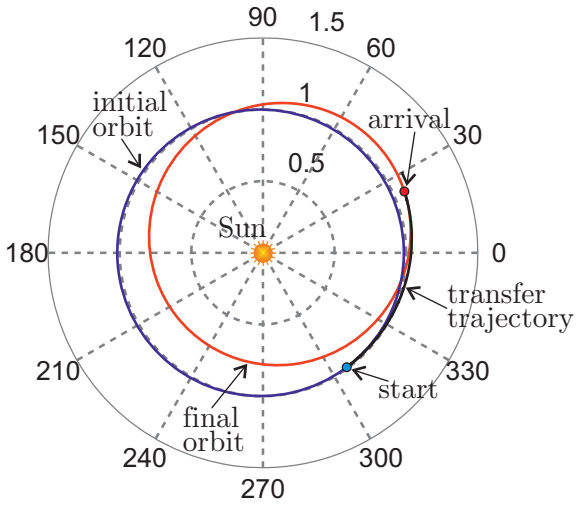


Figure 9: Optimal Earth-Apophis trajectory.

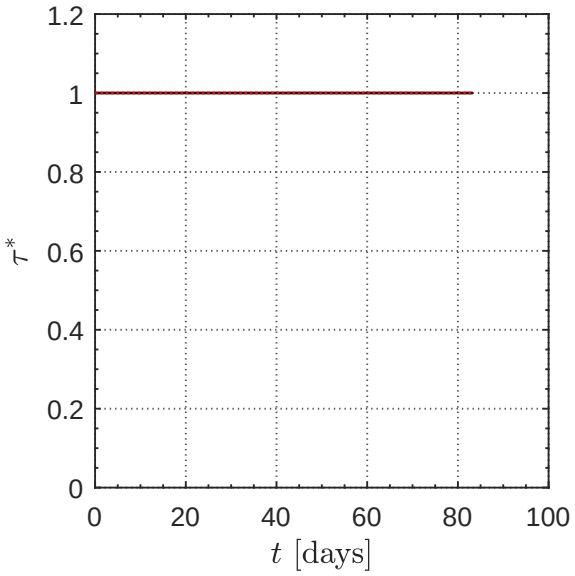


Figure 10: Earth-Apophis transfer: optimal control law $\tau^\star$ in the case of uncertainties in the value of $p_\oplus$ (solid line), and in the nominal case of constant $p_\oplus = \bar{p}_\oplus$ (dashed red line).

for the spacecraft to reach the target orbit.

## Conflict of interest statement

The authors declared that they have no conflicts of interest to this work.

## References

[1] M. Huo, G. Mengali, A. A. Quarta, Optimal planetary rendezvous with an electric sail, Aircraft Engineering and Aerospace Technology 88 (4) (2016) 512–522, doi: 10.1108/AEAT-01-2015-0012.

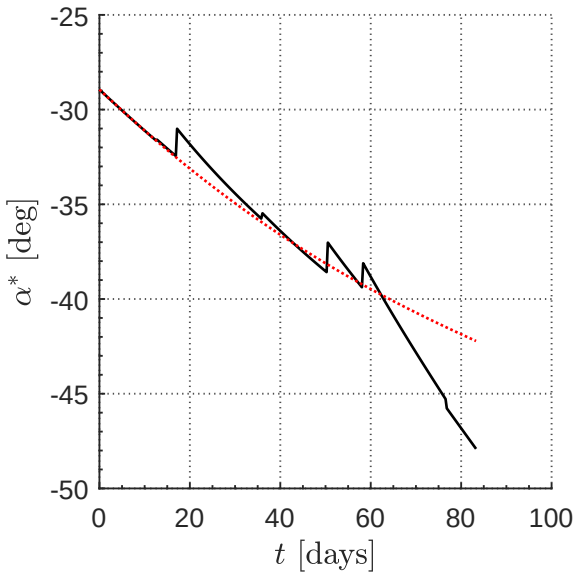


Figure 11: Earth-Apophis transfer: optimal control law $\alpha^\star$ in the case with uncertainties in the value of $p_\oplus$ (solid line), and in the nominal case of constant $p_\oplus = \bar{p}_\oplus$ (dashed red line).


[2] L. Niccolai, A. A. Quarta, G. Mengali, Electric sail-based displaced orbits with a refined thrust model, Proceedings of the Institution of Mechanical Engineers, Part G: Journal of Aerospace Engineering 232 (3) (2018) 423–432, doi: 10.1177/0954410016679195.

[3] A. A. Quarta, G. Mengali, Electric sail mission analysis for outer solar system exploration, Journal of Guidance, Control, and Dynamics 33 (3) (2010) 740–755, doi: 10.2514/1.47006.

[4] A. A. Quarta, G. Mengali, Minimum-time trajectories of electric sail with advanced thrust model, Aerospace Science and Technology 55 (2016) 419–430, doi: 10.1016/j.ast.2016.06.020.

[5] M. Bassetto, A. A. Quarta, G. Mengali, Locally-optimal electric sail transfer, Proceedings of the Institution of Mechanical Engineers, Part G: Journal of Aerospace Engineering 233 (1) (2019) 166–179, doi: 10.1177/0954410017728975.

[6] M. Huo, G. Mengali, A. A. Quarta, N. Qi, Electric sail trajectory design with Bezier curve-based shaping approach, Aerospace Science and Technology 88 (2019) 126–135, doi: 10.1016/j.ast.2019.03.023.

[7] L. Niccolai, A. A. Quarta, G. Mengali, Two-dimensional heliocentric dynamics approximation of an electric sail with fixed attitude, Aerospace Science and Technology 71 (2017) 441–446, doi: 10.1016/j.ast.2017.09.045.

[8] J. L. Phillips, S. J. Bame, A. Barnes, et al., Ulysses solar wind plasma observations from pole to pole, Geophysical Research Letters 22 (23) (1995) 3301–3304, doi: 10.1029/95GL03094.

[9] L. Gallana, F. Fraternale, M. Iovieno, S. M. Fosson, E. Magli, M. Opher, J. D. Richardson, D. Tordella, Voyager 2 solar plasma and magnetic field spectral analysis for intermedate data sparsity, Journal of Geophysical Research: Space Physics 121 (5) (2016) 3905–3919, doi: 10.1002/2015JA021830.

[10] G. Vulpetti, A critical review on the viability of a space propulsion based on the solar wind momentum flux, Acta Astronautica 32 (9) (1994) 641–644, doi: 10.1016/0094-5765(94)90074-4.

[11] J. M. Sokół, M. Bzowski, M. Tokumaru, K. Fujiki, D. J. McComas, Heliolatitude and time variations of solar wind structure from in situ measurements and interplanetary scintillation observations, Solar Physics 285 (1-2) (2013) 167–200, doi: 10.1007/s11207-012-9993-9.

[12] L. Niccolai, A. Anderlini, G. Mengali, A. A. Quarta, Impact of solar wind fluctuations on electric sail mission design, Aerospace Science and Technology 82-83 (2018) 38–45, doi: 10.1016/j.ast.2018.08.032.

[13] L. Niccolai, A. Anderlini, G. Mengali, A. A. Quarta, Electric sail displaced orbit control with solar wind uncertainties, Acta Astronautica 162 (2019) 563–573, doi: 10.1016/j.actaastro.2019.06.037.

[14] D. Gonzáles-Arribas, M. Soler, M. Sanjurjo-Rivo, Robust aircraft trajectory planning under wind uncertainty using optimal control, Journal of Guidance, Control, and Dynamics 41 (3) (2018) 673–688, doi: 10.2514/1.G002928.

[15] C. Greco, M. Di Carlo, M. Vasile, R. Epenoy, An intrusive polynomia algebra multiple shooting approach to the solution of optimal control problem, in: 69th International Astronautical Congress, Bremen, Germany, 2018.

[16] I. M. Ross, R. J. Proulx, M. Karpenko, Unscented optimal control for orbital and proximity operations in an uncertain environment: A new zermelo problem, in: AIAA/AAS Astrodynamics Specialist Conference 2014, San Diego, CA; United States, 2014, paper AIAA 2014-4423.

[17] Z. J. Sun, Y. Z. Luo, P. di Lizia, F. Bernelli Zazzera, Nonlinear orbital uncertainty propagation with differential algebra and gaussian mixture model, Science China: Physics, Mechanics and Astronomy 62 (3) (2019) 034511.1–034511.11, doi: 10.1007/s11433-018-9267-6.

[18] M. Huo, G. Mengali, A. A. Quarta, Electric sail thrust model from a geometrical perspective, Journal of Guidance, Control,

and Dynamics 41 (3) (2018) 734–740, doi: 10.2514/1.G003169.
[19] P. K. Toivanen, P. Janhunen, Spin plane control and thrust vectoring of electric solar wind sail, Journal of Propulsion and Power 29 (1) (2013) 178–185, doi: 10.2514/1.B34330.
[20] P. K. Toivanen, P. Janhunen, Thrust vectoring of an electric solar wind sail with a realistic sail shape, Acta Astronautica 131 (2017) 145–151, doi: 10.1016/j.actaastro.2016.11.027.
[21] A. E. Bryson, Y. C. Ho, Applied Optimal Control, Hemisphere Publishing Corporation, New York, NY, 1975, Ch. 2, pp. 71–89, ISBN: 0-891-16228-3.
[22] D. F. Lawden, Optimal Trajectories for Space Navigation, Butterworths & Co., London, 1963, Ch. 3, pp. 54–60.
[23] L. F. Shampine, M. K. Gordon, Computer Solution of Ordinary Differential Equations: The Initial Value Problem, W. H. Freeman, San Francisco, 1975, Ch. 10.
[24] L. F. Shampine, M. W. Reichelt, The MATLAB ODE suite, SIAM Journal on Scientific Computing 18 (1) (1997) 1–22, doi: 10.1137/S1064827594276424.
[25] P. Janhunen, A. A. Quarta, G. Mengali, Electric solar wind sail mass budget model, Geoscientific Instrumentation, Methods and Data Systems 2 (1) (2013) 85–95, doi: 10.5194/gi-2-85-2013.